HEAT TRANSFER ANALYSIS AND MODELING FOR A COAXIAL SOLAR COLLECTOR IN A DOMESTIC COGENERATION SYSTEM

Fabrizio Alberti[1,†], Luigi Crema[1] and Alberto Bertaso[1]

[1] Renewable Energies and Environmental Technology, Fondazione Bruno Kessler, 38123 Povo, Trento (Italy)

[†] corresponding author, email: alberti@fbk.eu

1. Introduction

The need for efficient energy generation in domestic houses push the research toward innovative system, that can efficiently cogenerate electrical and thermal power for heating and cooling. A good electrical conversion rate can be achieved when an energy source (hot sink) can reach temperatures of at least 250 °C. Both conventional and renewable sources can be used to run a domestic cogeneration system; they can be in the form of fossil fuels, biomass and solar energy.

This paper presents the analysis for a domestic solar concentration system, that is intended to be coupled with a Stirling cogeneration unit. The proposed solar collector consists of an array of linear reflecting parabolas housed on a small tracking system (Fig. 1), which focuses solar radiation on a series of vacuum tubes. The heat is transferred to thermal oil suitable for operating at medium-high temperatures and finally to the heat exchanger of a Stirling engine (Fig. 2). An example for such solar configuration has been developed by the Digespo project (Digespo, 2010).

Fig. 1: An example of concentrating optics with a East-West tracking system

In most vacuum glass-tubes today, the fluid inlet and outlet are both located on the same side in order to reduce cost, possible failures and losses. Consequently internal pipes can be configured in two distinct ways; either a U-pipe configuration (Fig. 3a) wherein the pipe is bent at the end, or as a coaxial configuration (Fig. 3b) that allows for a pipe-in-pipe design; where the latter option is deemed easier to realize since there is just one rather than two glass penetrations.

However the coaxial tube may still have some limiting factors with respect to functionality and efficiency. The temperatures profiles and the heat transfer distribution may suffer from cross-conduction phenomena between inlet and outlet flow, which generates an internal thermal coupling, and a non-linear maximum temperature distribution along the pipe. This phenomenon, which can happen under certain fluid dynamic condition, has been reported in literature (Glembin et al., 2010) as one of the limiting factors of thermal efficiency. A low flow rate is identified in Glembin's work as the main factor that can lead to strong internal coupling and the appearance of maximum temperatures located within the outer pipe rather than at the tube outlet. The presence of a maximum temperature differing from the outlet temperature causes higher radiative losses from the absorber layer, a heat transfer effect which is particularly noticed when operating at high temperature. The distinctive temperature profile and the increase of turnaround temperatures with respect to the outlet temperature is shown also by Kim et al. (2007) and Han et al. (2008), who respectively developed a one-dimensional numerical model and detailed 3-D simulations for all-glass vacuum tubes with a coaxial conduit.

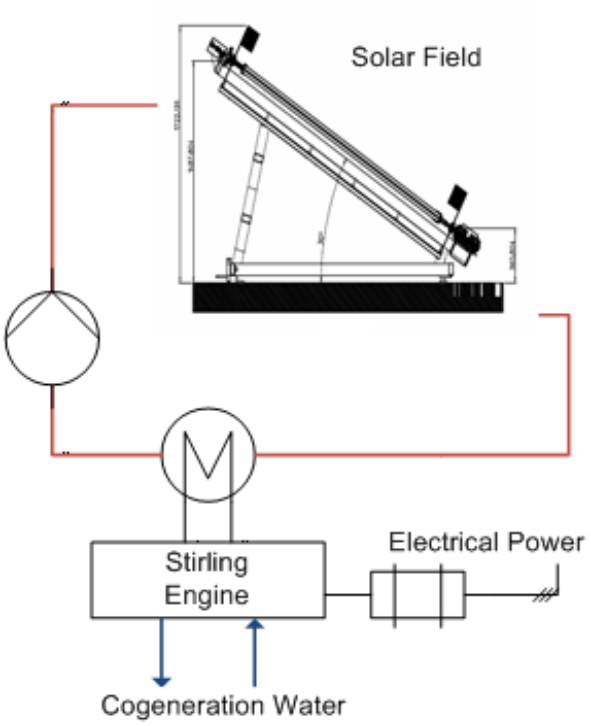

Fig. 2: Cogeneration system layout

Internal thermal coupling can also create a risk of exceeding the boiling temperature for conventional water collectors (Glembin et al, 2010). The same risk can also occur when thermal oils are used, since those fluids have a maximum bulk and film temperature. Such temperatures should be carefully controlled and not exceeded in order to preserve the fluid properties and performances.

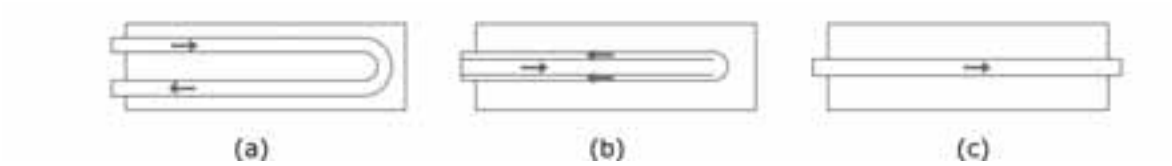

Fig. 3: Types of vacuum tube collectors: (a) U-pipe configuration, (b) coaxial configuration, (c) conventional parabolic trough

The aim of this work is to analyse the main parameters which influence the temperature profile and efficiency of a small-scale medium-high temperature solar concentrating array when a coaxial configuration is utilized, by taking into account the influence of internal thermal coupling. For this purpose a model is developed and presented. The model describes the main energy fluxes, and is capable of representing the spatial temperature profiles. It simulates in details thermodynamics, by coupling radiative, convective and conductive heat transfer with the fluid dynamics, both for laminar and turbulent flow. The model is adapted from previous works in the field of concentrating solar collectors (Forristall, 2003) and covers the research gap in domestic concentrating systems that use thermal oil as the heat transfer fluid. The theoretical approach that is followed has been validated during field monitoring on bigger parabolic trough by Price et al. (2006) and Burkholder and Kutscher (2009).

2. Theoretical model and parameters for the solar collector

A theoretical two dimensional model was developed and programmed to describe the temperature profile of a coaxial collector tube coupled with a solar concentrating system. Previous research (Glembin et al., 2010) has modeled heat losses with linear correlation, thus properly estimating irradiative losses only for temperatures ranges typical of domestic heating waters system. Others model (Forristall, 2003) have been developed specifically for receivers at higher temperatures, but they can be used to model only classical parabolic trough (Fig. 3c), and are therefore not suitable to capture the nonlinearity arising from coaxial configurations.

2.1. Heat Fluxes

The pipe is divided in N computational cells connected along the axis (Fig. 4). A steady-state energy balance is performed at every computational cell, from which temperatures and heat transfers can be calculated, along with heat transfer coefficients and fluid physical proprieties. In Fig. 5 a section of the pipe is presented for a generic computation cell, along with the points where temperatures and heat transfer are defined. The innermost temperature is the bulk temperature of the fluid in the inside tube (T_{1ave}), while the outermost temperature represent the glass outer surface (T_8). The returning flow in the section is identified by T_{4ave}. The temperature for the absorber coated surface is T_6; temperature for the cover glass are T_8 and T_7. Temperature of ambient (T_{AMB}) and temperature for the sky (T_{SKY}) are also defined, and will be used during the calculation. The subscript "ave" states that temperatures and other proprieties for the fluid (density, velocity, thermal capacity) are averaged between the outlet and inlet section of each cell.

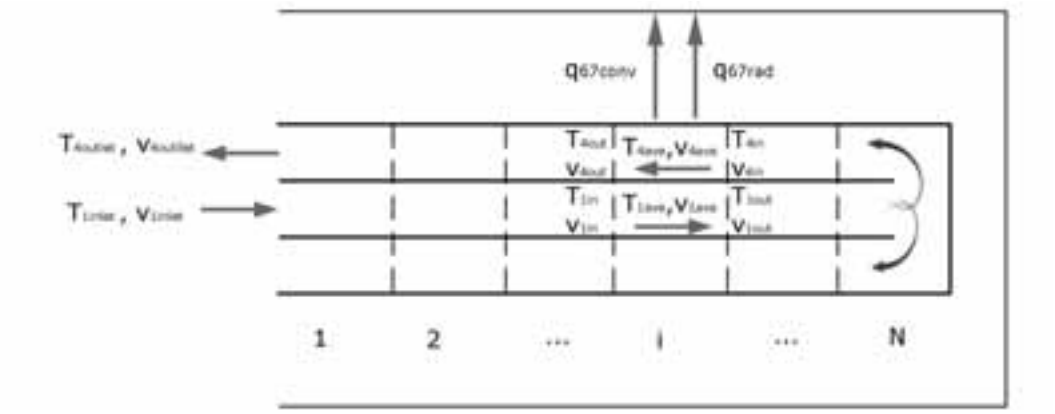

Fig. 4: Schematic of the two-dimensional heat transfer model. The list of heat fluxes and variable in the image is not exhaustive.

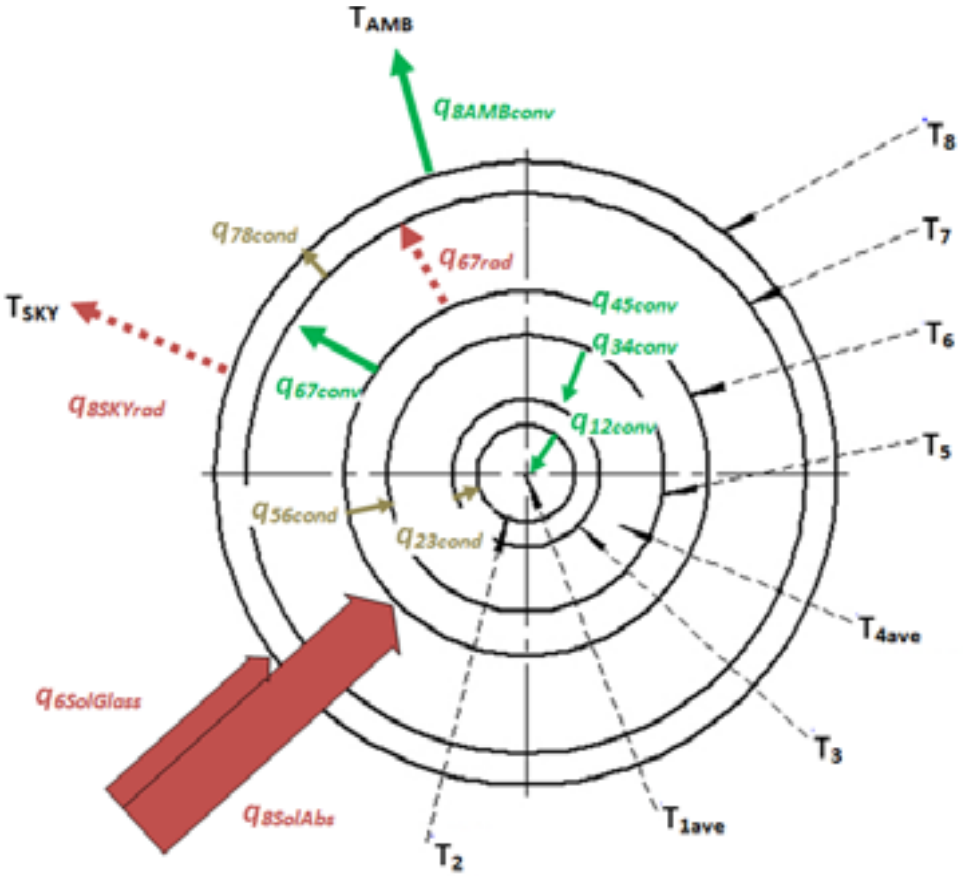

Fig. 5: Temperatures, thermal resistances and heat fluxes on a collector cross-section

Tab. 1 below provides the definition for each of the heat fluxes involved and specifies the temperature nodes. Tab. 2 show explicitly the variables used to calculate heat fluxes.

Tab. 1: Heat flux definitions

Heat Flux [W/m]	Heat Transfer Mode	Heat Transfer Path	
		From	To
$q_{8SolGlass}$	Solar irradiation absorption	incident solar irradiation	T_8: outer glass envelope surface
$q_{6SolAbs}$	Solar irradiation absorption	incident solar irradiation	T_6: outer absorber pipe surface
q_{12conv}	convection	T_{1ave}: heat transfer fluid	T_2: inner pipe, inner surface
q_{23cond}	conduction	T_2: inner pipe, inner surface	T_3: inner pipe, outer surface
q_{34conv}	convection	T_3: inner pipe, outer surface	T_{4ave} : heat transfer fluid
q_{45conv}	convection	T_{4ave}: heat transfer fluid	T_5 : annulus, inner surface
q_{56cond}	conduction	T_5: annulus, inner surface	T_6: absorber surface
q_{67rad}	radiation	T_6: absorber surface	T_7: inner glass surface
q_{67conv}	convection	T_6: absorber surface	T_7: inner glass surface
q_{78cond}	conduction	T_7: inner glass surface	T_8: outer glass surface
$q_{8SKYrad}$	radiation	T_8: outer glass surface	T_{SKY}: sky temperature
$q_{8AMBconv}$	convection	T_8: outer glass surface	T_{AMB}: ambient temperature

Stainless steel will be used as the test material within the tubes, since copper is not recommended due to the high temperatures reached in system. Conductivity for the stainless steel tubes is assumed to be a function of temperature (Eq. 1). Thermal conductivity in the glass is assumed to be constant, with a value of 1 $W\,m^{-1}K^{-1}$.

$$k = 0{,}013\,T + 15{,}2 \qquad \text{(Eq. 1)}$$

To model the convective heat transfer from the absorber to the heat transfer fluid for turbulent and transitional cases (Reynolds number > 2300) the correlation developed by Gnielinski (1976) is used. The remainder convective heat transfer coefficients defined in Tab. 2 are calculated with the following Nusselt number correlations: q_{67conv} with Ratzel et al. (1979) when pressure in the glass annulus is < 1 Torr and Raithby and Holland's correlation for natural convection in annular space when pressure is > 1 Torr (Bejan, 1995); for $q_{8AMBconv}$ natural convection is used in absence of wind while forced convection is used when the wind is simulated on the glass envelope (Incropera and DeWitt, 2007). A detailed discussion over the assumption and validity beyond those correlations can be find in Forristall (2003) and Incropera and DeWitt (2007).

2.2. Heat transfer fluid

The heat transfer fluid used in the model is thermal oil Therminol66, which is commonly used for thermal applications up to 345 °C. Thermal and physical proprieties implemented in the model can be found in Solutia (2010). Both on the inner and outer pipe, the bulk temperature for the fluid (T_{4ave} and T_{1ave}) should not exceed 345 °C, in order to preserve its thermochemicaly proprieties. Another limit is the film temperature

(T_5), which is the maximum temperature experienced by the fluid in contact with the absorber pipe. Film temperature is calculated by the ratio of the heat flux density to the heat transfer coefficient. When the heat flux density is very high, which is the case in a solar concentrating system, there is the risk to exceed the film temperature, even if the measured bulk temperature is under its limit. Although very little fluid is present in the film, if the film temperature exceeds the maximum recommended, the contribution to the degradation of that fluid volume can be high.

Tab. 2: Heat flux equations and variables

Heat Flux [W/m]	Equation	Variable Definitions
$q_{8SolGlass}$	$\rho_{conc} \cdot \alpha_{glass} \cdot G_b \cdot A_{aperture}$	ρ_{conc} = optical efficiency for the concentration system
		α_{glass} = glass absorbance
		G_b = solar beam irradiance
		$A_{aperture}$ = collector aperture
		L = collector length
$q_{6SolAbs}$	$\rho_{conc} \cdot \tau_{glass} \cdot \alpha_{Abs} \cdot G_b \cdot A_{aperture}$	α_{Abs} = absorber layer absorbance
		τ_{glass} = glass optical transmittance
q_{12conv}	$q_{12conv} = h_{12} \cdot D_1 \cdot \pi(T_2 - T_1)$ $h_{12} = Nu_{D1}\frac{k_1}{D_1}$	h_{12} = convection heat transfer coefficient
		D_1 = inside diameter, inside pipe
		Nu_{D1} = Nusselt number
		k_1 = fluid thermal conductivity
q_{23cond}	$\frac{2\pi k_{23}(T_3 - T_2)}{\ln(D_1 - D_2)}$	k_{23} = steel thermal conductivity
		D_2 = outside diameter, inside pipe
q_{34conv}	Analogous to q_{12conv}	-
q_{45conv}	Analogous to q_{12conv}	-
q_{56cond}	Analogous to q_{23cond}	-
q_{67rad}	$\frac{\sigma\pi D_4(T_7^4 - T_6^4)}{\frac{1}{\varepsilon_{Abs}} + \frac{(1-\varepsilon_{glass})}{D_4(\varepsilon_{glass}D_5)}}$	σ = Stefan-Boltzmann constant
		D_4= outer absorber diameter
		D_5= inner glass envelope diameter
q_{67conv}	Analogous to q_{12conv}	-
q_{78cond}	Analogous to q_{23cond}	-
$q_{8AMBconv}$	Analogous to q_{12conv}	-
$q_{8SKYrad}$	$\sigma\pi D_6 \varepsilon_{glass}(T_8^4 - T_{SKY}^4)$	D_6= glass envelope outer diameter

2.3. Energy and mass balance

The energy balance equation for the steady-state are determined by conserving energy at each surface of the collector cross-section. The energy balance is imposed at every *i* cell. It should be noted that the heat flux defined below have unit [W/m]. The usual heat flux per unit of area [W/m^2] is returned when those flux are multiplied by the length ΔL of the computational cell.

For i=1 to i=N

$$q_{12conv}(i) = q_{23cond}(i) \quad \text{(Eq. 2a)}$$

$$q_{23cond}(i) = q_{34conv}(i) \quad \text{(Eq. 2b)}$$

$$q_{45conv}(i) = q_{56cond}(i) \quad \text{(Eq. 2c)}$$

$$q_{56cond}(i) = q_{6SolAbs} - q_{67rad}(i) - q_{67conv}(i) \quad \text{(Eq. 2d)}$$

$$q_{67conv}(i) + q_{67rad}(i) = q_{78cond}(i) \quad \text{(Eq. 2e)}$$

$$q_{78cond}(i) + q_{8SolGlass} = q_{8AMBconv}(\mathrm{i}) + q_{8SKYrad}(\mathrm{i}) \quad \text{(Eq. 2f)}$$

$$q_{12conv}(i) \cdot \Delta L = \dot{m} \cdot \left(Cp_{1ave}(i) \cdot (T_{1out}(i) - T_{1in}(i)) + \frac{1}{2}(v_{1out}^2(i) - v_{1in}^2(i)) \right) \quad \text{(Eq. 2g)}$$

$$(q_{45conv}(i) - q_{34conv}(i)) \cdot \Delta L = \dot{m} \cdot \left(Cp_{4ave}(i) \cdot (T_{4out}(i) - T_{4in}(i)) + \frac{1}{2}(v_{4out}^2(i) - v_{4in}^2(i)) \right) \quad \text{(Eq. 2h)}$$

The solar energy absorbed by the glass envelop ($q_{8SolGlass}$) and absorber selective coating ($q_{6SolAbs}$) are a fraction of the solar radiation which is focused on the receiver by the parabolic mirror. They doesn't carry the *i* prefix, since they are assumed to be constant all along the collector length. The last two equations represent an energy balance for the fluid inside the inner tube and in the annular tube, where kinetic energy is also accounted for. Variation in the fluid velocity from the inlet to the outlet of each computational cell is determined with the following mass balance:

$$v_{1out}(i) = \dot{m} \left(\rho_{1out}(i) \cdot \pi \left(\frac{D_1}{2} \right)^2 \right) \quad \text{(Eq. 3a)}$$

$$v_{4out}(i) = \dot{m} / \left(\rho_{4out}(i) \cdot \left(\pi \left(\frac{D_3}{2} \right)^2 - \pi \left(\frac{D_2}{2} \right)^2 \right) \right) \quad \text{(Eq. 3b)}$$

Fluid specific heat capacity Cp_{1ave} and Cp_{4ave} are assumed to depend from the temperature and are evaluated at the mean fluid temperature T_{1ave} and T_{4ave}, while density ρ_{1out} and ρ_{4out} are calculated from the temperature at the outlet of the cell, T_{1out} and T_{4out}. At each cell the following equations are applied to ensure consistency for fluid temperature and velocity along the axis:

$$T_{1in}(i+1) = T_{1out}(i) \quad \text{(Eq. 4a)}$$

$$v_{1in}(i+1) = v_{1out}(i) \quad \text{(Eq. 4b)}$$

$$T_{4in}(i-1) = T_{4out}(i) \quad \text{(Eq. 4c)}$$

$$v_{4in}(i-1) = v_{4out}(i) \quad \text{(Eq. 4d)}$$

In terms of temperature and velocity the imposed boundary condition for the inlet fluid are:

$$T_{1in}(1) = T_{1inlet} \quad \text{(Eq. 5a)}$$

$$v_{1in}(1) = v_{1inlet} \quad \text{(Eq. 5b)}$$

Due to the nonlinearities in the model an iterative procedure is required to obtain the solution of this system of equation. The calculation ends when the convergence condition is verified. Segmentation in 100 elements is deemed to be a good compromise between numerical precision and computing time.

Finally, efficiency is calculated with equation Eq. 6.

$$efficiency_{Opt;Th} = \frac{\dot{m} \cdot Cp_{ave} \cdot (T_{1inlet} - T_{4outlet})}{G_b \cdot A_{aperture} \cdot L} \quad \text{(Eq. 6)}$$

2.4. Solar collector parameters

The typical variables used as an input for the model are presented in Tab. 3. The values for optical proprieties used during all the simulations have been chosen according to the target proposed within the Digespo project (2010), in the range of working temperatures from 250 °C to 350 °C (Tab. 4).

Tab. 3: Input variables

Input	Unit	Description
T_{linlet}	°C	Fluid temperature at inlet
v_{inlet}	m/s	Fluid velocity at inlet
G_b	W/m^2	Beam Irradiance on collector aperture
T_{AMB}	°C	Ambient Temperature

Tab. 4: Optical proprieties description and assumed values

Optical proprieties	Value	Description
ε_{Abs}	0,05	Selective coating emissivity
ε_{Glass}	0,9	Glass envelope emissivity
α_{Abs}	0,95	Selective coating absorbance
α_{Glass}	0,02	Glass envelope absorbance
τ_{glass}	0,97	Glass envelope transmittance
ρ_{conc}	0,9	Parabola and tracking system optical efficiency

The solar tube collector and the concentration optics have been given constructive characteristics and dimensions typical for a domestic application (Tab. 5); each parabola has the same length as the solar receiver and an aperture of 40 cm; the concentration ratio for the system is 11.

Tab. 5: Geometrical characteristics and assumed values

Geometrical Characteristic	Value [mm]	Description
D_1	8	Inner pipe, outer diameter
s_{12}	0,3	Inner pipe thickness
D_4	12	Annulus outer diameter
s_{34}	0,5	Annulus thickness
D_6	55,7	Glass envelope outer diameter
s_{56}	1,8	Glass envelope thickness
L	2	Collector length
$A_{aperture}$	400	Concentrator parabola aperture
C	11	Concentration Ratio

2.5. Simplification assumptions

The procedure described above leads to the heat transfer balance and temperature profile for a single solar collector. The proposed system is to be arranged with the tubes in a parallel configuration. The analysis of a single tubes is thus sufficient to characterize the whole system. The following assumptions are being made to the proposed model:

- The model calculates steady-state condition and thermal capacity are not accounted for.
- The solar flux on the receiver tube is assumed to be constant around the circumference, even if in reality the parabola reflects the radiation mainly on the lower section of the absorber tube.
- The optical efficiency for the parabola and tracking system is assumed to be constant at 0,9. The influence of the incident angle on the optical proprieties is not included, since the solar radiation is always assumed to be perpendicular to the receiver aperture.

- The model neglects thermal conduction within the pipe material along the tube axis. The same assumptions is made in the models developed by Glembin et al. (2010) and Forristall (2003).
- Thermal losses from the support fin clips of real tubes are not accounted for.
- Optical proprieties in the model do not depend on temperature; they are always assumed to be constant.
- The model can simulate laminar and turbulent flow on the inner and outer tube. However, the effect of redirection of the fluid at the turnaround is not modeled. The model thus slightly underestimate the turbulence in this position.

3. Results and Discussion

3.1. Flow influence on collector performance and temperature profile

The model described computes the temperature profile in a coaxial vacuum tube. The collector efficiency is here calculated when the inlet fluid velocity and consequently the flow rare is varied. During the simulation all the other parameters have been keep constant, while fluid inlet velocity is varied within the range indicated in Tab. 6. The flow rate can be derived from inlet velocity with equation:

$$\dot{m} = v_{1inlet} \cdot \pi \cdot (D_1/2)^2 \cdot \rho_{1inlet} \qquad \text{(Eq. 7)}$$

The collector aperture is assumed to intercept an irradiance of 1000 W/m^2, which is then concentrated on the absorber surface. The collector area for the simulated collector receiver is calculated as follow:

$$A_{collector} = L \cdot A_{aperture} \qquad \text{(Eq. 8)}$$

The collector performance is analysed with fluid entering in the collector at 300 °C, which corresponds to the returning temperature from the Stirling engine heat exchanger.

Tab. 6: Parameters used in simulations

Input	Unit	Value
T_{1inlet}	°C	300 °C
T_{AMB}	°C	20 °C
P_{ann_torr}	Torr	0,0001
v_{1inlet}	m/s	from 0,01 to 1

Fig. 6 show that efficiency drops quickly when a fluid inlet velocity below 0,1 m/s is imposed. Efficiency is about 80% at 0,1 m/s onwards, and it slightly increases after 0,4 m/s, when a turbulent flow regime is established both on the inner tube and in the annulus.

A turbulent flow increases the value for the heat transfer coefficient and is responsible for better heat exchange between the fluid and the absorber. The flow at the inner pipe becomes turbulent when the inlet fluid velocity is at 0,1 m/s, while the same effect occurs in the annulus when inlet fluid velocity exceed 0,4 m/s. The annulus and the inner pipe can show different flow regime at the same time, due to different hydraulic radius.

Efficiency decreases when the flow rate is reduced below a certain limit, due to temperature increases in the absorber. Fig. 7 and 8 present the temperature profiles versus path length x (which is the ratio of the distances from the tube connection to the overall tube length) for the case when the concentration is not applied, and the solar incident radiation on the absorber surface is assumed to be 1000 W/m^2. In Fig. 7 the inlet velocity is 0,1 m/s. The temperatures continuously rise from inlet to outlet. The maximum temperature is achieved at the outlet, where the fluid exits at 305 °C and the temperature on the absorber is close to 310 °C. Fig. 8 show the temperature profiles for a lower inlet velocity. The fluid in the annulus decreases in temperature when approaching the outlet since part of the heat absorbed is passing to the inner flow. This phenomena is known as internal thermal coupling, and should be avoided, since under this condition the maximum temperatures are located in the middle of the pipe. The absorber temperature (T_6) exceeds 360 °C in this zone, causing greater radiation losses compared to the case in Fig. 7. Another problem is related to the

thermal fluid maximum working temperature (T_{4ave}, T_5), which are exceeded inside the collector, even if the outlet temperature is below the limit of 345 °C.

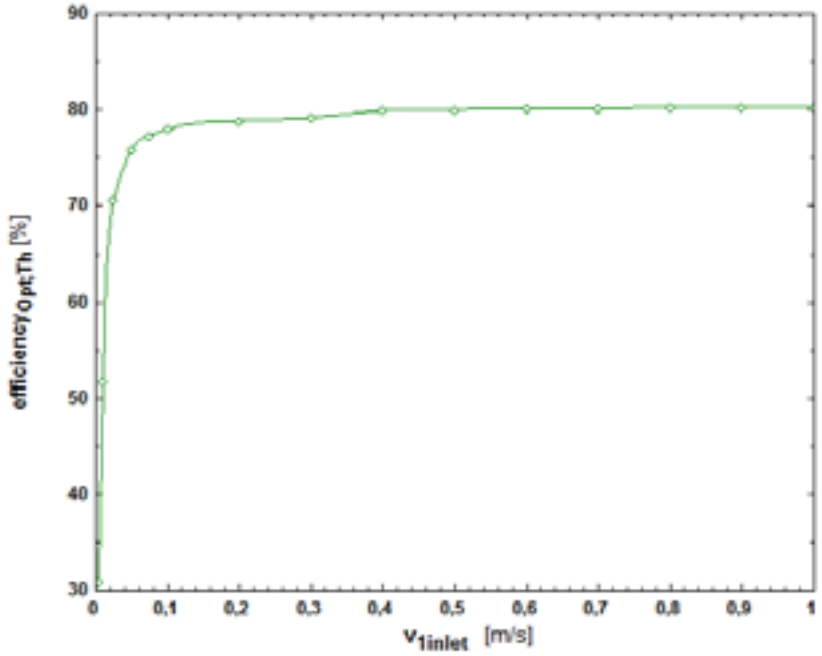

Fig. 6: Efficiency versus fluid inlet velocity

The internal thermal coupling would not be observed in a U-pipe configuration, since the two flows are not in thermal contact through the internal walls. In this case a continuous temperature increase is established for any flow rate. The effect of internal thermal coupling shown in Fig. 8 is less important compared with the results from Glembin et. al (2010), which studied this phenomena using water as the thermal fluid; this is explained by a lower thermal conductivity of the thermal oil compared to the one of water. Thermal conductivity of the fluid seems to be the most important parameter which affect the magnitude of the phenomena.

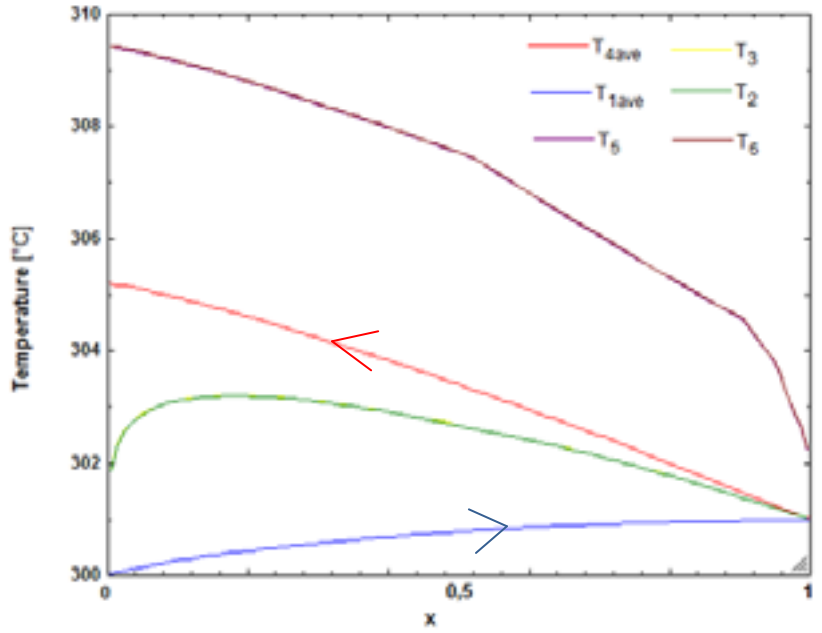

Fig. 7: Temperature profile for v_{1inlet} = 0,1 m/s. Fluid bulk temperature (T_{1ave}; T_{4ave}); film temperature (T_5; T_2); absorber temperature (T_6)

In Fig. 9 the maximum bulk and film temperature funded under different flows regime are shown. The film and bulk temperature are kept below their limit when an inlet velocity of 0,4 m/s is imposed. It can be concluded that a minimal flow rate should be carefully guaranteed, in order to avoid fluid deterioration inside

the collector. Increasing the flow rate over this limit does not improve thermal efficiency (Fig. 6) and can only lead to greater pumping losses. Since these collector are intended to be part of an electrical generation system, the electrical consumption for the pump should also be optimized and kept at the minimum value possible.

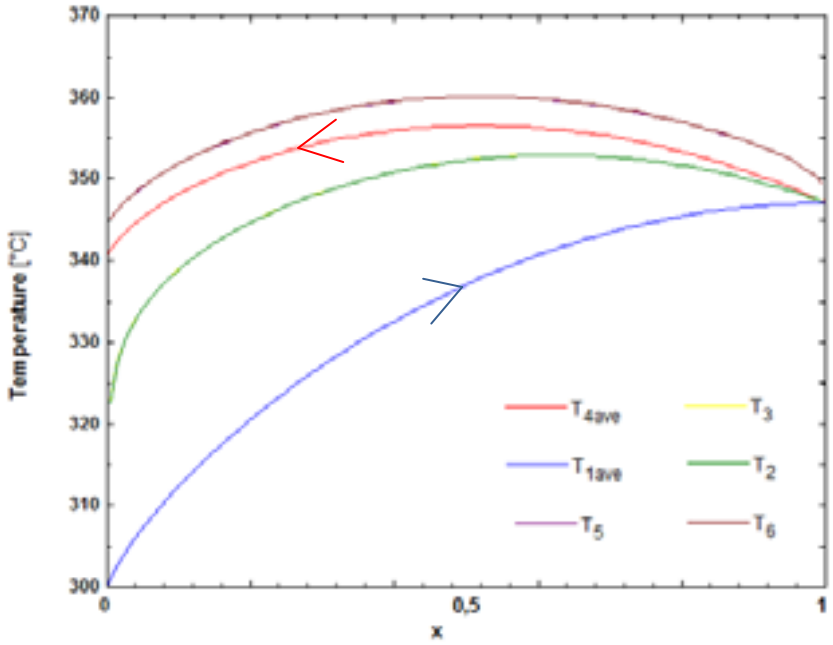

Fig. 8: Temperature profile for v_{1inlet} = 0,01 m/s. Fluid bulk temperature (T_{1ave}; T_{4ave}); film temperature (T_5; T_2); absorber temperature (T_6)

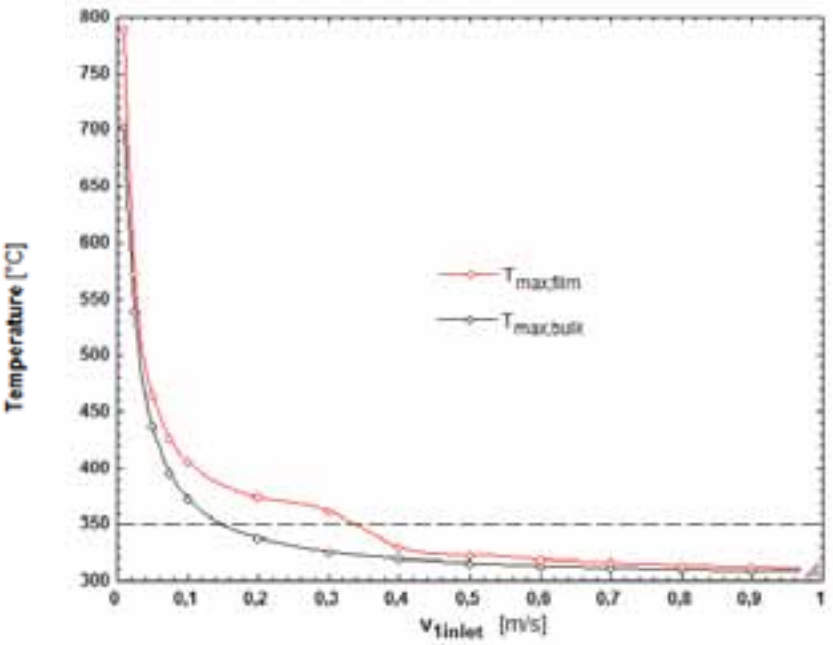

Fig. 9: Maximum film and bulk temperature for the fluid inside the collector, as a function of inlet velocity. The fluid is entering in the collector with a temperature of 300 °C. The dashed line represent the maximum allowable temperature (345 °C) for thermal oil

3.2. Pressure losses in the vacuum annulus

The vacuum in the annulus between the absorber and the glass envelope is fundamental for good collector performance. A raise in pressure can affect directly the heat transfer coefficient and the convective heat flux between the absorber and the inner glass surface (q_{67conv}).

Collector efficiency is analyzed in this section when pressure is lost in the annulus, and air is assumed to

enter in the vacuum space. The reference case is a collector with concentration optics that are exposed to 1000 W/m^2 of solar radiation and a inlet velocity of 0,4 m/s (Tab. 7).

Tab. 7: Parameters used in simulations

Input	Unit	Value
T_{1inlet}	°C	300
v_{inlet}	m/s	0,4
G_b	W/m^2	1000
T_{AMB}	°C	20
P_{ann_torr}	Torr	From 10^{-7} to 10^4

Efficiency is plotted in Fig. 10 when pressure in the annulus is varied from 10^{-7} to 10^4 Torr. Results show that the vacuum level is a parameter that strongly affects efficiency. Any gasses entering in this space can deteriorate the performance, which rapidly drops when the value of 0,0001 Torr (0,013 Pa) is exceeded.

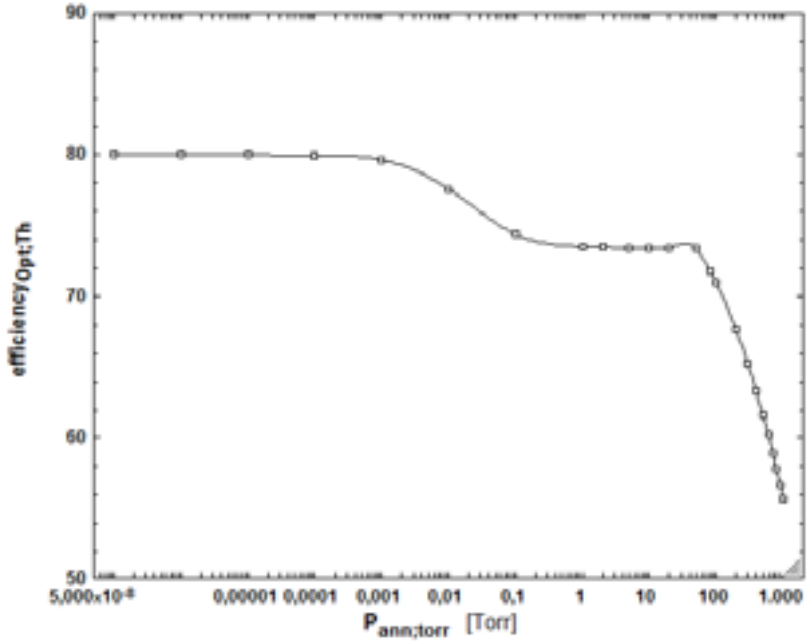

Fig. 10: Efficiency versus different pressure in the vacuum annulus. Efficiency start to drop when the pressure in the annulus as reached 0,0001 Torr (0,013 Pa)

This value is confirmed by experimental data obtained under similar conditions by Mientkewitz et al. (2011). This report show a stabilization in stagnation temperatures when the vacuum is better than 0,01 Pa, meaning that an optimal condition is achieved and a better vacuum gives no advantages in terms of receiver effectiveness.

4. Conclusion

In this paper a proposed cogeneration unit coupled with a small-scale concentration solar system is presented. The advantages and problems associated to the use of coaxial vacuum tubes as the receiver is then discussed. A computer program was developed to calculate the temperature profiles while considering the internal heat exchange between the inner and outer pipe.

Its capability was used to investigate the influence of flow rate on efficiency and temperature profiles. Results indicate that a minimum flow rate should be imposed in order to avoid efficiency losses and the exceeding of temperature limits within the tube.

The efficiency has been shown to be strongly depend on the quality of the vacuum inside the glass envelope

and a pressure limit is individuated. The theoretical result funded by means of simulations agree well with experimental data obtained independently.

Acknowledgements

The work presented in this paper has partially been realized within the Digespo project (http://www.digespo.eu), which is funded by the research program of the European Commission, under the topic FP-7 Energy. A special thanks goes to Brian Restall (Pim, Malta), for the support in reviewing and editing the text.

References

Bejan, A., 1995. Convection Heat Transfer, Second Edition. New York, NY: John Wiley and Sons.

Burkholder, F., Kutscher, C., 2009. Heat Loss Testing of Schott's 2008 PTR70 Parabolic Trough Receiver. Technical Report NREL/TP-550-45633. NREL; May 2009.

Digespo Project, 2010. http://www.digespo.eu. Website with information and updates, last visited 10/08/2011

Forristall, R., 2003. Heat transfer analysis and modeling of a parabolic trough solar receiver implemented in Engineering equation Solver. Technical Report NREL/TP-550-34169. NREL; October 2003.

Glembin, J., Rockendorf, G., Scheuren, J., 2010. Internal thermal coupling in direct-flow coaxial vacuum tube collectors. Solar Energy 84, 1137–1146

Gnielinski, V., 1976. New Equations for Heat and Mass Transfer in Turbulent Pipe and Channel Flow. International Chemical Engineering 16, 359–363.

Han, H., Kim, J.T., Ahn, H.T., Lee, S.J., 2008. A three dimensional performance analysis of all-glass vacuum tubes with coaxial fluid conduit. International Communications in Heat and Mass Transfer 35, 589–596.

Incropera, F., DeWitt, D., 2007. Fundamentals of Heat and Mass Transfer, Fifth Edition. New York, NY: John Wiley and Sons.

Kim, J.T., Ahn, H.T., Han, H., Kim, H.T., Chun, W., 2007. The performance simulation of all-glass vacuum tubes with coaxial fluid conduit. International Communications in Heat and Mass Transfer 34, 587–597.

Mientkewitz, G., Hesse, S., Schaffrath, W., 2011. Definition of the evacuated solar tube. Deliverable D2.3, Digespo Project, FP7-Energy-2009-1, EU.

Price, J., Forristall, R., Wendelin, T., Lewandowski, A., 2006. Field survey of parabolic trough receiver thermal performance. Proceedings of ISEC2006, ASME International Solar Energy Conference. July 8-13, 2006, Denver, Colorado, USA.

Ratzel, A., Hickox, C., Gartling, D., 1979. Techniques for Reducing Thermal Conduction and Natural Convection Heat Losses in Annular Receiver Geometries. Journal of Heat Transfer 101, 108–113.

Solutia, 2010. Therminol66 Fluid Proprieties. Information Bulletin, Group Provoc T.B.S 10-7 12/98 E.